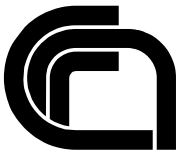

*Consiglio Nazionale delle Ricerche*

# Stopping rules for iterative methods in nonnegatively constrained deconvolution

P. Favati, G. Lotti, O. Menchi, F. Romani

IIT TR-15/2011

**Technical report**

**Luglio 2011**

**Istituto di Informatica e Telematica**

# Stopping rules for iterative methods in nonnegatively constrained deconvolution

P. Favati G. Lotti O. Menchi F. Romani

July 8, 2011

**Abstract**

We consider the two-dimensional discrete nonnegatively constrained deconvolution problem, whose goal is to reconstruct an object $\mathbf{x}^*$ from its image $\mathbf{b}$ obtained through an optical system and affected by noise. When the large size of the problem prevents regularization by filtering, iterative methods enjoying semiconvergence property, coupled with suitable strategies for enforcing nonnegativity, are suggested. For these methods an accurate detection of the stopping index is essential. In this paper we analyze various stopping rules and test their effect on three different iterative regularizing methods, by a large experimentation.

## 1 Introduction

We consider here the following two-dimensional discrete deconvolution problem: reconstruct an object $\boldsymbol{x}^*$ from its image $\boldsymbol{b}$ measured through an imaging system represented by a known matrix $A$. In addition to the blurring introduced by the optical system, $\boldsymbol{b}$ is affected by the noise $\boldsymbol{\eta}$ due to the detector device. The model for this problem is

$$A\boldsymbol{x}^* = \boldsymbol{b} - \boldsymbol{\eta}, \tag{1}$$

where each component $b_i$ of $\boldsymbol{b}$ is taken as the realization of a Poisson random variable with expected value $(A\boldsymbol{x}^*)_i$, to which an uncorrelated Gaussian white noise with variance $\sigma^2$ is added, i.e.

$$\boldsymbol{b} = \text{Poisson}(A\boldsymbol{x}^*) + N(0, \sigma^2 I). \tag{2}$$

This model takes into account both the noise due to the fluctuations in the counting process of the acquisition of the image which obeys to Poisson statistics, and the readout noise, due to imperfections of the recording device, which obeys to Gaussian statistics [3]. Important fields of application are the deconvolution of astronomical images taken by a telescope and the deconvolution of medical and microscopy images.

Nonnegativity constraints are imposed by the physical nature of the problem. Hence $A$, $\boldsymbol{x}^*$, $\boldsymbol{b}$ and the reconstructed image are assumed to be nonnegative. Generally $A$ is a large ill-conditioned matrix. Because of the presence of the noise, the vector $A^\dagger \boldsymbol{b}$, solution of the system $A\boldsymbol{x} = \boldsymbol{b}$, may differ much from $\boldsymbol{x}^*$. Hence regularization is required, coupled with suitable strategies for enforcing nonnegativity. When the large size of the problem prevents regularization by filtering, iterative regularization methods enjoying the semiconvergence property are suggested. With these methods the computed iterations $\mathbf{x}^{(k)}$ first approach $\mathbf{x}^*$, then go away and the choice of the index at which the iteration should be stopped is critical. Ideally, the iteration should be stopped when the solution error $\|\mathbf{x}^{(k)} - \mathbf{x}^*\|$ is minimum, but this is clearly impracticable.

In this paper we examine two classes of stopping rules. In the first class, rules based on predictive error estimates CGV and UPRE are considered. They are derived from the parameter choice methods for regularization by filtering (see for example [4, 14] for a thorough comparison) and require the knowledge of the trace of the influence matrix. In the second class, some rules based on the discrepancy principle are considered in both the standard form and the compensated version, which uses the trace of the influence matrix. Our aim is to analyze the behavior of the two classes of stopping rules in connection with three descent methods which enforce nonnegativity and have different step size characteristics. A difficulty with iterative methods is that, in general, the influence matrix is not explicitly known. To overcome this drawback, we follow [1, 13] which suggest the use of the Trace Lemma (see Chap. 7 in [15]). In this way the matter is shifted to the randomized environment. The resulting rules can be considered only heuristics, since the Trace Lemma is applied after a sequence of approximations, without formally checking if the hypotheses are really fulfilled. We will examine the validity of this heuristics through the experimentation.

The paper is so organized: Section 2 presents the likelihood functions used in the minimization, Section 3 describes the considered descent methods. Each method corresponds to an influence matrix, whose trace plays an important role in the stopping rules. In the case of iterative methods the influence matrix cannot be explicitly expressed and its trace must be approximated. Two different approaches for this approximation are described in Section 4. The chosen stopping rules are described in Section 5. The computational costs are listed in Section 6. Finally, the results of the experiments are shown in Section 7.

Assumptions and notations: in the following we assume that $A$ is generated by a positive space invariant bandlimited PSF and that periodic boundary conditions are set, resulting in a 2-level circulant matrix $A$. Hence the convolutions $A\boldsymbol{x}$ or $A^T\boldsymbol{x}$, which provides the major part of the computational cost of the methods, can be easily computed by means of FFT. We

assume also that both $A\boldsymbol{x} > \mathbf{0}$ and $A^T\boldsymbol{x} > \mathbf{0}$ for any $\boldsymbol{x} \geq \mathbf{0}$ with $\boldsymbol{x} \neq \mathbf{0}$. Moreover, the variance $\sigma^2$ may or may not be known, and this knowledge may or may not be incorporated in the algorithms we will use. For simplicity, the multiplication and the division between vectors, denoted by the symbols $\odot$ and $\oslash$, are defined componentwise. The notation $\|\cdot\|$ is used for the Euclidean norm.

## 2 The likelihood function

To find a regularized solution of (1), one can minimize a suitable likelihood function, which in general takes into account the nature of the noise. The likelihood function to be considered in the case of Poisson noise is the Kullback-Leibler divergence

$$\ell(\boldsymbol{x}, \boldsymbol{b}) = \sum\nolimits_i \Big( (A\boldsymbol{x})_i - b_i + b_i \log \frac{b_i}{(A\boldsymbol{x})_i} \Big), \tag{3}$$

whose minimizers are the points $\widehat{\boldsymbol{x}} \geq \mathbf{0}$ satisfying

$$\widehat{x}_i \, \frac{\partial \ell(\boldsymbol{x}, \boldsymbol{b})}{\partial x_i}\Big|_{\boldsymbol{x}=\widehat{\boldsymbol{x}}} = 0 \quad \text{and} \quad \frac{\partial \ell(\boldsymbol{x}, \boldsymbol{b})}{\partial x_i}\Big|_{\boldsymbol{x}=\widehat{\boldsymbol{x}}} \geq 0 \quad \text{if} \quad \widehat{x}_i = 0. \tag{4}$$

The derivatives $\dfrac{\partial \ell(\boldsymbol{x}, \boldsymbol{b})}{\partial x_i}$ are the components of the gradient of $\ell(\boldsymbol{x}, \boldsymbol{b})$, which in our case is

$$\boldsymbol{g}(\boldsymbol{x}) = A^T \Big( (A\boldsymbol{x} - \boldsymbol{b}) \oslash A\boldsymbol{x} \Big). \tag{5}$$

As seen in (2), both Poisson and Gaussian components contribute to the noise, but for large values of the argument $\lambda$ the Poisson distribution is well approximated by a normal distribution, i.e. Poisson$(\lambda) \approx \mathcal{N}(\lambda, \lambda)$. Then for a sufficiently large $A\boldsymbol{x}^*$ it is possible to express $\boldsymbol{\eta}$ as a Gaussian random noise of zero mean, i.e.,

$$\boldsymbol{b} = A\boldsymbol{x}^* + \boldsymbol{\eta}, \quad \text{where} \quad \boldsymbol{\eta} = \mathcal{N}(0, H) \text{ with } H = \operatorname{diag}(A\boldsymbol{x}^* + \boldsymbol{\sigma}^2), \tag{6}$$

where $\boldsymbol{\sigma}^2 = \sigma^2 \boldsymbol{e}$ and $\boldsymbol{e}$ is the vector of all ones. Then the level of the noise is estimated through the expected value

$$\mathcal{E}\Big( \|\boldsymbol{\eta}\|^2 \Big) = \operatorname{tr} H = \sum\nolimits_i (A\boldsymbol{x}^*)_i + N\sigma^2, \tag{7}$$

where tr $H$ denotes the trace of $H$ and $N$ is the size of the problem, i.e. $N = n^2$ is the number of the pixels of the $n \times n$ image.

Conversely, adding $\boldsymbol{\sigma}^2$ to both sides of (6), we get [3]

$$\boldsymbol{\beta} = \boldsymbol{b} + \boldsymbol{\sigma}^2 \approx \text{Poisson}(A\boldsymbol{x}^* + \boldsymbol{\sigma}^2). \tag{8}$$

In this way, $\boldsymbol{\beta}$ is seen as the realization of a Poisson random variable with expected value $\boldsymbol{\mu} = A\boldsymbol{x}^* + \boldsymbol{\sigma}^2$.

In [5] Chap. 7, it is shown that in the case of a Gaussian noise like the one in (6), the problem of finding a regularized solution of (1) is equivalent to finding the minimum of the following generalized discrepancy functional

$$\ell_H(\boldsymbol{x}, \boldsymbol{b}) = \frac{1}{2} \|H^{-1/2}(A\boldsymbol{x} - \boldsymbol{b})\|^2.$$

For a practical use, we approximate $A\boldsymbol{x}^*$ in $H$ by $\boldsymbol{b}$, obtaining the functional

$$\widehat{\ell}(\boldsymbol{x}, \boldsymbol{b}) = \frac{1}{2} \|W^{1/2}(A\boldsymbol{x} - \boldsymbol{b})\|^2, \quad \text{with} \quad W = \operatorname{diag}\Big(\boldsymbol{e} \oslash (\boldsymbol{b} + \boldsymbol{\sigma}^2)\Big), \tag{9}$$

which can be regarded as a weighted quadratic approximation of $\ell(\boldsymbol{x}, \boldsymbol{b})$ (see [2]). The gradient of $\widehat{\ell}(\boldsymbol{x}, \boldsymbol{b})$ is

$$\widehat{\boldsymbol{g}}(\boldsymbol{x}) = A^T W (A\boldsymbol{x} - \boldsymbol{b}) = A^T \Big((A\boldsymbol{x} - \boldsymbol{b}) \oslash (\boldsymbol{b} + \boldsymbol{\sigma}^2)\Big), \tag{10}$$

a linearized approximation of $\boldsymbol{g}(\boldsymbol{x})$ (see [3]).

## 3 Iterative regularization methods

When the large size of the problem prevents regularization by filtering, a frequently used technique consists in employing an iterative regularization method. Starting from an initial point $\boldsymbol{x}^{(0)}$ the method computes a sequence $\boldsymbol{x}^{(k)}$ aiming at the minimization of the likelihood function. Due to the presence of the noise, after a certain number of iterations, say $K$, the points $\boldsymbol{x}^{(k)}$ are corrupted and stop to approach $\boldsymbol{x}^*$. At that point the iteration must be interrupted. The approximation $\boldsymbol{x}_K$ of $\boldsymbol{x}^*$ is the so-called *regularized* solution.

The iterative methods used in this case are mostly descent methods, particularly suited to deal with nonnegativity. In [8] the performance of some methods of this type, belonging to the SGP (Scaled Gradient Projection) class, has been analyzed from various points of view. We consider here three of them, which have been found the most efficient ones for both the reconstruction accuracy and the convergence speed in the 2D case. Starting from a nonnegative $\boldsymbol{x}^{(0)}$, the iteration computes

$$\boldsymbol{x}^{(k+1)} = \boldsymbol{x}^{(k)} + \boldsymbol{\lambda}^{(k)} \odot \boldsymbol{p}^{(k)}, \quad \text{subjected to} \quad \boldsymbol{x}^{(k+1)} \geq \boldsymbol{0}, \tag{11}$$

where, according to (4), the descent direction is

$$\boldsymbol{p}^{(k)} = -\boldsymbol{x}^{(k)} \odot \boldsymbol{g}^{(k)}, \quad \text{with} \quad \boldsymbol{g}^{(k)} = \boldsymbol{g}\,(\boldsymbol{x}^{(k)}). \tag{12}$$

The vector $\boldsymbol{\lambda}^{(k)}$ of the step sizes characterizes the method. Three choices are feasible: a vector independent from $\boldsymbol{x}^{(k)}$ (possibly scalar), a scalar vector dependent on $\boldsymbol{x}^{(k)}$, a nonscalar vector dependent on $\boldsymbol{x}^{(k)}$.

• The first method is EM (*Expectation Maximization*), obtained by setting in (11) $\boldsymbol{\lambda}^{(k)} = \boldsymbol{e}/\boldsymbol{c}$, where $\boldsymbol{c} = A^T\boldsymbol{e}$ is the vector of the sums by column of $A$. The method is applied in the form

$$\boldsymbol{x}^{(k+1)} = \boldsymbol{x}^{(k)} \oslash \boldsymbol{c} \odot A^T \Big(\boldsymbol{b} \oslash A\boldsymbol{x}^{(k)}\Big). \tag{13}$$

• The second method is WMRNSD (*Weighted Modified Residual Norm Steepest Descent*) [3], obtained by replacing $\boldsymbol{g}^{(k)}$ with $\widehat{\boldsymbol{g}}^{(k)}$ in (12). The scalar step size minimizes $\widehat{\ell}(\boldsymbol{x}, \boldsymbol{b})$ along the direction $\boldsymbol{p}^{(k)}$ and is suitably reduced to guarantee that $\boldsymbol{x}^{(k+1)}$ has no negative components, i.e.

$$\boldsymbol{\lambda}^{(k)} = m_k\boldsymbol{e}, \quad \text{with} \quad m_k = \min\Big( -\frac{\widehat{\boldsymbol{g}}^{(k)^T}\boldsymbol{p}^{(k)}}{\|W^{1/2}A\boldsymbol{p}^{(k)}\|^2}\,, \frac{1}{\max_i\ \widehat{g}_i^{(k)}}\Big)$$

(the constant $m_k$ is positive since $\boldsymbol{p}^{(k)}$ is a descent direction).

• The third method is obtained by setting $\boldsymbol{p}^{(k)}$ as in (12). It can be seen as a generalization of EM and will be called here SGP (actually in [7], where this method is defined, the term SGP indicates a whole class of methods, which depend on various parameters. The parameters chosen for the present method are those identifying SGP-PcB in [8]). For the vector of step sizes consider the parameter

$$\alpha_k = \frac{\boldsymbol{s}^{(k)T}\boldsymbol{z}^{(k)}}{\|\boldsymbol{z}^{(k)}\|^2}, \quad \text{where} \quad \boldsymbol{s}^{(k)} = \boldsymbol{x}^{(k)} - \boldsymbol{x}^{(k-1)},\ \boldsymbol{z}^{(k)} = -(\boldsymbol{p}^{(k)} - \boldsymbol{p}^{(k-1)}),$$

bounded to be positive, and the vector $\boldsymbol{h}^{(k)}$, whose $i$th component is equal to $\alpha_k$ if $\alpha_k g_i^{(k)} < 1$ and to $1/g_i^{(k)}$ otherwise. Then $\boldsymbol{\lambda}^{(k)} = \overline{\lambda}\,\boldsymbol{h}^{(k)}$, where $\overline{\lambda}$ minimizes $\ell(\boldsymbol{x}^{(k)} + \lambda\boldsymbol{h}^{(k)} \odot \boldsymbol{p}^{(k)}, \boldsymbol{b})$ varying $\lambda \in (0, 1]$. Since $\ell(\boldsymbol{x}, \boldsymbol{b})$ is not quadratic, an approximate line-search must be performed, for example by applying the Armijo rule (see [7, 8] for the details). If $\boldsymbol{x}^{(k)} \geq \boldsymbol{0}$, the bound $\lambda \leq 1$ guarantees that $\boldsymbol{x}^{(k+1)} \geq \boldsymbol{0}$.

WMRNSD and SGP can be seen as generalizations of EM. Usually generalizations aim at improving the convergence rate, but in a regularization context a better convergence rate may result in a poorer reconstruction accuracy. Actually, the experiments in [8] have shown that in the 2D case WMRNSD averagely outperforms EM for both the reconstruction accuracy and the convergence rate, while SGP is faster than the other two methods but slightly less accurate.

A simple choice suggested in [13] for $\boldsymbol{x}^{(0)}$, which cannot be chosen equal to $\boldsymbol{0}$, is $\boldsymbol{x}^{(0)} = A^T\boldsymbol{b}$. This is the vector we adopt in the experiments.

## 4 The influence matrix

For any $k$, let $R_k$ be the *regularization matrix*, i.e. the matrix which, applied to the right-hand side, would produce the $k$th iterate $\boldsymbol{x}^{(k)} = R_k\,\boldsymbol{b}$. The matrix $A_k = AR_k$ is called the *influence matrix*. Many regularization methods make use of information about the influence matrix to determine acceptable values of the parameters involved in the stopping procedures. In the case of an iterative regularizing method, the influence matrix is not explicitly known but, given a vector $\boldsymbol{v}$, it is possible to approximate the components of the vector $A_k\boldsymbol{v}$, in the following way.

The matrix $R_k$ depends not only on $k$, but also on $\boldsymbol{b}$. Since $R_k\mathbf{0} = \mathbf{0}$, where $\mathbf{0}$ is the null vector, at the first order $R_k$ can be approximated by the Jacobian matrix $\widehat{R}_k(\boldsymbol{b})$, whose $(j,h)$th element is $(\widehat{R}_k(\boldsymbol{b}))_{(j,h)} = \dfrac{\partial x_j^{(k)}}{\partial b_h}$, and $x_j^{(k)}$ can be approximated by $\sum_h \dfrac{\partial x_j^{(k)}}{\partial b_h}\, b_h^{(k)}$. The $j$th component of the vector $\boldsymbol{w}^{(k)} = \widehat{R}_k(\boldsymbol{b})\boldsymbol{v}$ is given by

$$w_j^{(k)} = \sum\nolimits_h \frac{\partial x_j^{(k)}}{\partial b_h}\, v_h, \tag{14}$$

and the vector $\boldsymbol{w}^{(k)}$, the directional derivative of $\boldsymbol{x}^{(k)}$ along the vector $\boldsymbol{v}$, is assumed as an approximation of $R_k\,\boldsymbol{v}$, setting $A_k\boldsymbol{v} = A\boldsymbol{w}^{(k)}$. To compute it, we consider two procedures, whose effectiveness will be compared in the experiments. The first procedure, here called $\mathbf{P}_1$, is based on an analytical process. It is the one suggested in [13] for EM and in [1] for WMRNSD.

- Procedure $\mathbf{P}_1$: using (11) the following recursive relation for $\boldsymbol{w}^{(k)}$ can be obtained

$$w_j^{(k+1)} = w_j^{(k)} + \sum\nolimits_h \frac{\partial\,(\lambda_j^{(k)} p_j^{(k)})}{\partial b_h}\, v_h.$$

Except in the case of EM where $\lambda_j^{(k)}$ is a constant with respect to $\boldsymbol{b}$, the computation of these derivatives is unfeasible, and $\boldsymbol{w}^{(k)}$ must be approximated. Then we assume the step sizes $\boldsymbol{\lambda}^{(k)}$ to be so slowly varying with respect to $\boldsymbol{b}$ to be considered a constant. From (12) it follows that

$$w_j^{(k+1)} = w_j^{(k)} + \lambda_j^{(k)} \sum\nolimits_h \frac{\partial\, p_j^{(k)}}{\partial b_h}\, v_h = w_j^{(k)} - \lambda_j^{(k)} \left( g_j^{(k)}\, w_j^{(k)} + x_j^{(k)} \sum\nolimits_h \frac{\partial g_j^{(k)}}{\partial b_h}\, v_h \right).$$

From (5) we have

$$g_j^{(k)} = c_j - \sum\nolimits_i a_{i,j}\, \frac{b_i}{(A\boldsymbol{x}^{(k)})_i}\,,$$

hence

$$\sum\nolimits_h \frac{\partial g_j^{(k)}}{\partial b_h}\, v_h = -\sum\nolimits_h \Big( a_{h,j}\, \frac{1}{(A\boldsymbol{x}^{(k)})_h} - \sum\nolimits_i a_{i,j}\, \frac{b_i}{(A\boldsymbol{x}^{(k)})_i^2} \sum\nolimits_r a_{i,r} \frac{\partial x_r^{(k)}}{\partial b_h} \Big) v_h$$

$$= -\sum\nolimits_i a_{i,j}\, \frac{1}{(A\boldsymbol{x}^{(k)})_i} \Big( v_i - \frac{b_i}{(A\boldsymbol{x}^{(k)})_i} \sum\nolimits_r a_{i,r} w_r^{(k)} \Big).$$

An analogous relation holds when $\boldsymbol{g}^{(k)}(\boldsymbol{x})$ is replaced by $\widehat{\boldsymbol{g}}^{(k)}(\boldsymbol{x})$ for method WMRNSD. In this case, from (10) we have

$$\widehat{g}_j^{(k)} = \sum\nolimits_i a_{i,j} \Big( \frac{(A\boldsymbol{x}^{(k)})_i + \sigma^2}{b_i + \sigma^2} - 1 \Big),$$

hence

$$\sum\nolimits_h \frac{\partial \widehat{g}_j^{(k)}}{\partial b_h}\, v_h = -\sum\nolimits_h a_{h,j}\, v_h\, \frac{(A\boldsymbol{x}^{(k)})_h + \sigma^2}{(b_h + \sigma^2)^2} + \sum\nolimits_i a_{i,j}\, \frac{1}{b_i + \sigma^2} \sum\nolimits_r a_{i,r}\, w_r^{(k)}$$

$$= -\sum\nolimits_i a_{i,j}\, \frac{1}{b_i + \sigma^2} \Big( v_i\, \frac{(A\boldsymbol{x}^{(k)})_i + \sigma^2}{b_i + \sigma^2} - \sum\nolimits_r a_{i,r}\, w_r^{(k)} \Big).$$

So we have

$$\boldsymbol{w}^{(k+1)} = \boldsymbol{w}^{(k)} - \boldsymbol{\lambda}^{(k)} \odot \boldsymbol{q}^{(k)}, \tag{15}$$

where for EM and SGP

$$\boldsymbol{q}^{(k)} = \boldsymbol{w}^{(k)} \odot \boldsymbol{g}^{(k)} - \boldsymbol{x}^{(k)} \odot A^T \Big( \boldsymbol{v} \oslash A\boldsymbol{x}^{(k)} \,-\, \boldsymbol{b} \odot A\boldsymbol{w}^{(k)} \oslash (A\boldsymbol{x}^{(k)})^2 \Big),$$

and for WMRNSD

$$\boldsymbol{q}^{(k)} = \boldsymbol{w}^{(k)} \odot \widehat{\boldsymbol{g}}^{(k)} - \boldsymbol{x}^{(k)} \odot A^T W \Big( \boldsymbol{v} \odot W(A\boldsymbol{x}^{(k)} + \sigma^2) \,-\, A\boldsymbol{w}^{(k)} \Big)$$

(in [1] the vector $\boldsymbol{v} \odot W(A\boldsymbol{x}^{(k)} + \sigma^2)$ is replaced by $\boldsymbol{v}$).

The step sizes $\boldsymbol{\lambda}^{(k)}$ are those computed at the $k$th iteration of the method. Hence the vectors $\boldsymbol{w}^{(k)}$ are computed from $\boldsymbol{v}$ in the same way as the vectors $\boldsymbol{x}^{(k)}$ are computed from $\boldsymbol{b}$. Having chosen $\boldsymbol{x}^{(0)} = A^T\boldsymbol{b}$, we take $\boldsymbol{w}^{(0)} = A^T\boldsymbol{v}$.

The assumption made on the step sizes which has allowed us to derive the recursive expressions (15) for computing $\boldsymbol{w}^{(k)}$ might not be satisfied when WMRNSD or SGP are used. For this reason a second procedure, called $\mathbf{P}_2$, which does not require this assumption, is here suggested.

- Procedure $\mathbf{P}_2$: an alternative way to compute $\boldsymbol{w}^{(k)}$ can be devised by applying the Taylor formula to $x_j^{(k)} = x_j^{(k)}(\boldsymbol{b})$, seen as a function of $\boldsymbol{b}$. Then

$$x_j^{(k)}(\boldsymbol{b} + \delta\, \boldsymbol{v}) = x_j^{(k)}(\boldsymbol{b}) + \sum\nolimits_h \frac{\partial x_j^{(k)}}{\partial b_h}\Big|_{\boldsymbol{b}} \delta\, v_h + O(\delta^2),$$

where $\delta$ is a small constant, leading to an approximation of the directional derivative (14) by a difference quotient

$$\sum_h \frac{\partial x_j^{(k)}}{\partial b_h} v_h \approx \frac{x_j^{(k)}(\boldsymbol{b} + \delta\, \boldsymbol{v}) - x_j^{(k)}(\boldsymbol{b})}{\delta}.$$

So we set

$$\boldsymbol{w}^{(k)} = \frac{\boldsymbol{x}^{(k)}(\boldsymbol{b} + \delta\, \boldsymbol{v}) - \boldsymbol{x}^{(k)}(\boldsymbol{b})}{\delta}. \tag{16}$$

To apply this formula, we need the vector $\boldsymbol{x}^{(k)}(\boldsymbol{b} + \delta\, \boldsymbol{v})$, which is computed by applying the chosen method (11) to the right-hand side vector $\boldsymbol{b} + \delta\, \boldsymbol{v}$. This means a double computation: at each iteration the two vectors $\boldsymbol{x}^{(k)}$ and $\boldsymbol{x}^{(k)}(\boldsymbol{b}+\delta\boldsymbol{v})$ should be computed in parallel, the first one starting from $\boldsymbol{x}^{(0)} = A^T\boldsymbol{b}$ and the second one starting from $\boldsymbol{x}^{(0)}(\boldsymbol{b}+\delta\, \boldsymbol{v}) = A^T(\boldsymbol{b}+\delta\, \boldsymbol{v})$. Since the truncation error of the approximation is of order $O(\delta^2)$, it is appropriate to choose $\delta \sim \epsilon^{1/2}$, where $\epsilon$ is the unit roundoff of the arithmetic.

In the experiments only procedure $\mathbf{P}_1$ will be applied with EM, while both procedures $\mathbf{P}_1$ and $\mathbf{P}_2$ will be applied with WMRNSD and SGP, to determine how much the dependance of $\boldsymbol{\lambda}^{(k)}$ on $\boldsymbol{b}$ influences the correctness of $\boldsymbol{w}^{(k)}$. Anyway, we must note that procedure $\mathbf{P}_2$ is applicable to any method, bypassing the difficulty of computing analytically the derivative of $\boldsymbol{w}^{(k)}$.

# 5 Finding the optimal index

The three methods considered in the previous section enjoy the semiconvergence property, i.e. the computed iterations $\boldsymbol{x}^{(k)}$ first approach $\boldsymbol{x}^*$, then go away. Hence the index $k$ can be considered the *regularization parameter* and the choice of the index $K$ at which the iteration should be stopped is critical. Ideally, the iteration should be stopped when the solution error $\epsilon^{(k)} = \|\boldsymbol{x}^{(k)} - \boldsymbol{x}^*\|$ is minimum. The objective is then finding the *optimal* index $K$. An early stopping of the iteration would give a too smooth reconstruction, whereas a late stopping would give artifacts due to large oscillations. A not too large overestimation of $K$ produces in general less damage, because the initial decrease of the error is more pronounced than the subsequent increase after the minimum.

Since the solution error is not directly computable, an acceptable approximation of $K$ is usually sought through the *predictive error* $\boldsymbol{\pi}^{(k)} = A\boldsymbol{x}^{(k)} - A\boldsymbol{x}^*$. Also this error is not directly computable, but there are techniques in the literature (see [15], Chapt. 7) which estimate $\boldsymbol{\pi}^{(k)}$ by means of the *residual* $\boldsymbol{r}^{(k)} = A\boldsymbol{x}^{(k)} - \boldsymbol{b}$. We consider here two stopping rules, GCV and UPRE, based on estimates of the predictive error. We consider also

a second group of stopping rules which exploit the discrepancy principle. Only GCV does not require statistical information about the noise.

In general, the stopping rules use information about the trace of the influence matrix, which is obtained by using the following
*Trace Lemma*: Given a symmetric matrix $B$ of size $N$ and a vector $\boldsymbol{v}$ of $N$ independent samples of a normal random variable with zero mean and variance $\sigma^2$, then

$$\sigma^2 \text{tr } B = \mathcal{E}(\boldsymbol{v}^T B \boldsymbol{v}),$$

where $\mathcal{E}$ denotes the expected value. If $\boldsymbol{v}$ has a covariance matrix $\mathbf{cov}(\boldsymbol{v}) = H$, with $H$ a diagonal matrix, then

$$\text{tr}\,(HB) = \mathcal{E}(\boldsymbol{v}^T B \boldsymbol{v}). \qquad \square$$

For a practical implementation, according to [15], the components of $\boldsymbol{v}$ are generated independently and take on the values $+1$ and $-1$ with equal probability $1/2$. From now on, by $\boldsymbol{v}$ we indicate always this particular vector. Applying the Trace Lemma to $A_k$, we have

$$\text{tr } A_k \approx \boldsymbol{v}^T A_k \boldsymbol{v} = \boldsymbol{v}^T A \boldsymbol{w}^{(k)}, \quad \text{where} \quad \boldsymbol{w}^{(k)} = R_k \boldsymbol{v}. \tag{17}$$

To compute $\boldsymbol{w}^{(k)}$ we use either (15) or (16).

### 5.1 Rules based on estimates of the predictive error

• *The Generalized Cross Validation (GCV).* The strong point of this technique is that it does not require the knowledge of $\sigma^2$, making it particularly suited to EM and SGP. First applied to regularization methods whose influence matrix is explicitly known, as Tikhonov method, it has been extended [1, 13] to iterative methods through the use of the Trace Lemma.

An estimate of the mean squared norm of the predictive error $\|\boldsymbol{\pi}^{(k)}\|^2$ is given by the GCV functional

$$GCV(k) = \frac{N\|\boldsymbol{r}^{(k)}\|^2}{[\text{tr}\,(I - A_k)]^2}\,. \tag{18}$$

The iteration should be stopped when $GCV(k)$ reaches the minimum (stopping rule $\mathbf{S}_1$). The denominator in (18) is computed using (17), then

$$\text{tr}\,(I - A_k) = N - \text{tr } A_k = N - \boldsymbol{v}^T A \boldsymbol{w}^{(k)}.$$

The quantity $N - \text{tr } A_k$ is considered as the effective number of degrees of freedom of the estimate.

Recognizing the minimum of $GCV(k)$ can be difficult if $\|\boldsymbol{r}^{(k)}\|^2$ is not a regularly decreasing function, but has a zigzag behavior, as it may happen

with WMRNSD. In this case we may resort to an estimate of the weighted predictive error $\|W^{1/2}\boldsymbol{\pi}^{(k)}\|^2$ by means of $\|W^{1/2}\boldsymbol{r}^{(k)}\|^2$. To find the correct number of degrees of freedom of this estimate, we note that $W^{1/2}\boldsymbol{r}^{(k)}$ can be viewed as the residual of $\boldsymbol{x}^{(k)}$ computed solving the preconditioned system

$$A'\boldsymbol{x} = \boldsymbol{b}', \quad \text{where} \quad A' = W^{1/2}A, \quad \boldsymbol{b}' = W^{1/2}\boldsymbol{b}.$$

The influence matrix is $A'_k = A'R'_k$, where

$$\boldsymbol{x}^{(k)} = R'_k\,\boldsymbol{b}' = R'_k\,W^{1/2}\boldsymbol{b}.$$

Then $R'_k\,W^{1/2} = R_k$ and $A'_k = A'R'_k = W^{1/2}AR_kW^{-1/2}$, hence tr $A'_k =$ tr $A_k$. The weighted GCV functional is then

$$GCV_W(k) = \frac{N\|W^{1/2}\boldsymbol{r}^{(k)}\|^2}{\left[\text{tr}\,(I - A_k)\right]^2}\,. \tag{19}$$

The iteration should be stopped when $GCV_W(k)$ reaches the minimum (stopping rule $\mathbf{S}_2$). The presence of $\sigma^2$ in (19) advises against the use of this weighted functional in connection with EM and SGP. At any rate, an ad-hoc experimentation is devoted to establish if it is worthwhile.

- *The Unbiased Predictive Risk Estimator (UPRE).* Since

$$\boldsymbol{r}^{(k)} = \boldsymbol{\pi}^{(k)} - \boldsymbol{\eta}, \quad \text{where} \quad \boldsymbol{\pi}^{(k)} = A\boldsymbol{x}^{(k)} - A\boldsymbol{x}^* = (A_k - I)A\boldsymbol{x}^* + A_k\boldsymbol{\eta},$$

then

$$\mathcal{E}(\|\boldsymbol{r}^{(k)}\|^2) = \mathcal{E}(\|\boldsymbol{\pi}^{(k)}\|^2) + \mathcal{E}(\|\boldsymbol{\eta}\|^2) - 2\,\mathcal{E}(\boldsymbol{\eta}^T\boldsymbol{\pi}^{(k)}),$$

where

$$\mathcal{E}(\boldsymbol{\eta}^T\boldsymbol{\pi}^{(k)}) = \mathcal{E}(\boldsymbol{\eta}^T(A_k - I)A\boldsymbol{x}^* + \boldsymbol{\eta}^T A_k\boldsymbol{\eta}) = \mathcal{E}(\boldsymbol{\eta}^T A_k\boldsymbol{\eta}),$$

because $\mathcal{E}(\boldsymbol{\eta}) = \mathbf{0}$. Then

$$\mathcal{E}(\frac{1}{N}\,\|\boldsymbol{\pi}^{(k)}\|^2) + \mathcal{E}(\frac{1}{N}\,\|\boldsymbol{\eta}\|^2) = \mathcal{E}(\frac{1}{N}\,\|\boldsymbol{r}^{(k)}\|^2) + \frac{2}{N}\,\mathcal{E}(\boldsymbol{\eta}^T A_k\boldsymbol{\eta}).$$

For (6), $\boldsymbol{\eta}$ can be viewed as a Gaussian random variable with zero mean and a covariance matrix $H = \text{diag}(A\boldsymbol{x}^* + \boldsymbol{\sigma}^2)$. By the Trace Lemma we have

$$\mathcal{E}(\boldsymbol{\eta}^T A_k\boldsymbol{\eta}) = \text{tr}\,(H\,A_k) = \mathcal{E}(\boldsymbol{v}^T H\,A_k\boldsymbol{v}) = \mathcal{E}(\boldsymbol{v}^T\text{diag}(A\boldsymbol{x}^* + \boldsymbol{\sigma}^2)A\boldsymbol{w}^{(k)}).$$

The approximation of $A\boldsymbol{x}^*$ by $\boldsymbol{b}$ leads to the definition of the UPRE functional

$$U(k) = \frac{1}{N}\,\|\boldsymbol{r}^{(k)}\|^2 + \frac{2}{N}\,(\boldsymbol{v}^T\text{diag}(\boldsymbol{b} + \boldsymbol{\sigma}^2)A\boldsymbol{w}^{(k)}). \tag{20}$$

The iteration should be stopped when $U(k)$ reaches the minimum (stopping rule $\mathbf{S}_3$).

As in the case of GCV, it may be difficult to find the minimum of $U(k)$ if $\|\boldsymbol{r}^{(k)}\|^2$ has a zigzag behavior. In this case a weighted functional should be considered instead of (20). From $W^{1/2}\boldsymbol{r}^{(k)} = W^{1/2}\boldsymbol{\pi}^{(k)} - W^{1/2}\boldsymbol{\eta}$ we get

$$\mathcal{E}(\frac{1}{N}\,\|W^{1/2}\boldsymbol{\pi}^{(k)}\|^2)+\mathcal{E}(\frac{1}{N}\,\|W^{1/2}\boldsymbol{\eta}\|^2) = \mathcal{E}(\frac{1}{N}\,\|W^{1/2}\boldsymbol{r}^{(k)}\|^2)+\frac{2}{N}\,\mathcal{E}(\boldsymbol{\eta}^T W A_k\boldsymbol{\eta}).$$

The random vector $\boldsymbol{\eta}$ has zero mean and a covariance matrix $H$, then by the Trace Lemma $\mathcal{E}(\boldsymbol{\eta}^T W A_k\boldsymbol{\eta}) = \mathcal{E}(\boldsymbol{v}^T HWA\boldsymbol{w}^{(k)})$. The approximation of $A\boldsymbol{x}^*$ by $\boldsymbol{b}$ leads to the definition of the weighted UPRE functional

$$U_W(k) = \frac{1}{N}\,\|W^{1/2}\boldsymbol{r}^{(k)}\|^2 + \frac{2}{N}\,(\boldsymbol{v}^T A\boldsymbol{w}^{(k)}). \tag{21}$$

The iteration should be stopped when $U_W(k)$ reaches the minimum (stopping rule $\mathbf{S}_4$).

### 5.2 Rules based on the discrepancy principle

According to the discrepancy principle, the optimal index $K$ is the one for which the norm of the residual $\|\boldsymbol{r}^{(K)}\|$ matches the noise level $\|\boldsymbol{\eta}\|$ of the data. Then, because of (7), the iteration should be stopped when

$$\|\boldsymbol{r}^{(k)}\|^2 \approx \sum\nolimits_i (A\boldsymbol{x}^*)_i + N\sigma^2.$$

For a practical implementation $A\boldsymbol{x}^*$ is replaced by $\boldsymbol{b}$, giving the

- stopping rule $\mathbf{S}_5$: $\quad\dfrac{1}{N}\,\|\boldsymbol{r}^{(k)}\|^2 \approx \dfrac{1}{N}\,\sum\nolimits_i b_i + \sigma^2.$

The discrepancy principle can be extended to the weighted residual $W^{1/2}\boldsymbol{r}^{(k)}$, which at the optimal index should match the weighted noise level of the data. By the Trace Lemma

$$\mathcal{E}(\|W^{1/2}\boldsymbol{\eta}\|^2) = \mathcal{E}(\boldsymbol{\eta}^T\,W\boldsymbol{\eta}) = \mathrm{tr}\,(HW) = \sum\nolimits_i \frac{(A\boldsymbol{x}^*)_i + \sigma^2}{b_i + \sigma^2}.$$

As above, $A\boldsymbol{x}^*$ is replaced by $\boldsymbol{b}$, giving the

- stopping rule $\mathbf{S}_6$: $\quad\dfrac{1}{N}\,\|W^{1/2}\boldsymbol{r}^{(k)}\|^2 \approx 1.$

Actually, as noted in [16], in our case the discrepancy principle should not be applied as stated above. In fact, the variance of the noise which affects the data is object dependent, against the assumption of a white Gaussian noise underlying the $\chi^2$ distribution on which the discrepancy principle is based. But a further extension can be considered, which takes into account the case of the Poisson noise. In fact, in [16] it is proved that if $\beta$ is a Poisson random variable with expected value $\mu$ and

$$F(\mu,\beta) = \mu - \beta + \beta\,\log\frac{\beta}{\mu}\,,$$

then

$$\mathcal{E}\Big(F(\mu,\beta)\Big) = \frac{1}{2} + O\Big(\frac{1}{\mu}\Big).$$

Applying this formula to each component of the vector $\boldsymbol{\beta}$ defined in (8), i.e. with $\beta_i = b_i + \sigma^2$ and $\mu_i = (A\boldsymbol{x}^*)_i + \sigma^2$, for sufficiently large $\mu_i$ we have

$$\mathcal{E}\Big((A\boldsymbol{x}^*)_i - b_i + (b_i+\sigma^2)\,\log\frac{b_i+\sigma^2}{(A\boldsymbol{x}^*)_i+\sigma^2}\Big) \approx \frac{1}{2}.$$

This expected value suggests how to extend the discrepancy principle to Poisson data. The discrepancy between the computed values $A\boldsymbol{x}^{(k)}$ and the observed data $\boldsymbol{b}$, which in the Gaussian case is measured by the residual, is now measured by the divergence

$$\ell_{\sigma^2}\Big(\boldsymbol{x}^{(k)},\boldsymbol{b}\Big) = \sum\nolimits_i \Big((A\boldsymbol{x}^{(k)})_i - b_i + (b_i+\sigma^2)\,\log\frac{b_i+\sigma^2}{(A\boldsymbol{x}^{(k)})_i+\sigma^2}\Big).$$

So we are led to the formulation of the

- stopping rule $\mathbf{S}_7$: $\dfrac{1}{N}\,\ell_{\sigma^2}\Big(\boldsymbol{x}^{(k)},\boldsymbol{b}\Big) \approx \dfrac{1}{2}.$

The three stopping rules $\mathbf{S}_5$, $\mathbf{S}_6$ and $\mathbf{S}_7$ share the same defect: they underestimate the optimal index. The reason is that they do not use the correct degrees of freedom, which is not $N$ but $N-\operatorname{tr} A_k$. As a remedy, *compensated* discrepancy principles are suggested (see [9, 14]). So we have

- stopping rule $\mathbf{S}_8$: $\dfrac{\|\boldsymbol{r}^{(k)}\|^2}{N-\operatorname{tr} A_k} \approx \dfrac{1}{N}\sum\nolimits_i b_i + \sigma^2,$
- stopping rule $\mathbf{S}_9$: $\dfrac{\|W^{1/2}\boldsymbol{r}^{(k)}\|^2}{N-\operatorname{tr} A_k} \approx 1,$
- stopping rule $\mathbf{S}_{10}$: $\dfrac{\ell_{\sigma^2}\Big(\boldsymbol{x}^{(k)},\boldsymbol{b}\Big)}{N-\operatorname{tr} A_k} \approx \dfrac{1}{2}.$

# 6 Computational costs

At each iteration the three methods EM, WMRNSD and SGP require one convolution by matrix $A$ and one convolution by matrix $A^T$ for the computation of $\boldsymbol{x}^{(k)}$ and $\boldsymbol{r}^{(k)}$. One more convolution is required by SGP for the approximate line search.

If rules $\mathbf{S}_5$, $\mathbf{S}_6$ or $\mathbf{S}_7$ are used, the trace of $A_k$ is not required. Otherwise, the computation of $\boldsymbol{w}^{(k)}$ requires two convolutions if procedure $\mathbf{P}_1$ is used, and doubles the cost of the method if procedure $\mathbf{P}_2$ is used. The convolution for the computation of $A\boldsymbol{w}^{(k)}$ required by the trace is not counted because $A\boldsymbol{w}^{(k)}$ is needed by $\boldsymbol{w}^{(k+1)}$ when (15) is used and is computed by subtracting

two $A\boldsymbol{x}^{(k)}$ values when (16) is used. Then the computational cost of EM and WMRNSD is 4 convolutions per iteration with both procedures $\mathbf{P}_1$ and $\mathbf{P}_2$ and the computational cost of SGP is 5 convolutions per iteration with procedure $\mathbf{P}_1$ and 6 convolutions per iteration with procedure $\mathbf{P}_2$.

To correctly evaluate the impact of these costs per iteration on the overall costs of the methods, it is convenient to have a rough idea of the relative convergence rates. To this aim, for each problem considered in the experiments of the next section we have found the ratios $\kappa_{EW} = K_E/K_W$, $\kappa_{WS} = K_W/K_S$ and $\kappa_{ES} = K_E/K_S$, where $K_E$, $K_W$ and $K_S$ are the optimal indices of the methods EM, WMRNSD and SGP respectively. On average, for all the problems we have obtained

$$\kappa_{EW}^{(av)} \sim 1.7, \quad \kappa_{WS}^{(av)} \sim 2.6, \quad \kappa_{ES}^{(av)} \sim 4.4,$$

confirming that SGP has the better convergence rate. The corresponding averages of the ratios of the solution errors are

$$\sigma_{EW}^{(av)} \sim 1.01, \quad \sigma_{WS}^{(av)} \sim 0.99, \quad \sigma_{ES}^{(av)} \sim 0.99,$$

showing that the reconstruction accuracy is minimally influenced by the chosen method.

# 7 Numerical experiments

The numerical experimentation, which has been conducted with *Mathematica*, deals with two images of astronomical interest (the spiral galaxy NGC 1288 [6] and an image of satellite [11]) and two of medical interest (the synthetic Shepp-Logan phantom [17] and a Hoffman phantom [10]), widely used in the literature for testing image deconvolution algorithms. The number of pixels is $N = 128^2$. The matrix $A$ which performs the blur is a 2-level circulant matrix generated by a positive space invariant bandlimited PSF with a bandwidth $\nu = 15$, normalized in such a way that the sum of the elements is equal to 1. We consider exponential PSFs of the following types.

(a) Gaussian PSFs represented by masks with entries

$$m_{i,j} = \exp(-\alpha\, i^2 - \beta j^2), \quad -\nu \le i, j \le \nu,$$

with the parameters

mask $M_1$ $\quad \alpha = 0.3, \quad \beta = 0.25;$ $\quad$ the condition number of $A$ is $\sim 10^4$,
mask $M_2$ $\quad \alpha = 0.1, \quad \beta = 0.1;$ $\quad$ the condition number of $A$ is $\sim 10^{11}$.

(b) Motion-type PSFs represented by masks with entries

$$m_{i,j} = \exp(-\alpha(i+j)^2 - \beta(i-j)^2), \quad -\nu \le i, j \le \nu,$$

with the parameters

| | | | |
|---|---|---|---|
| mask $M_3$ | $\alpha = 0.02$, | $\beta = 0.01$; | the condition number of $A$ is $\sim 10^6$, |
| mask $M_4$ | $\alpha = 0.04$, | $\beta = 0.02$; | the condition number of $A$ is $\sim 10^9$. |

The vectors $\boldsymbol{b}$ are generated according to (2), varying the intensity of the image in order to obtain different levels of the Poisson noise and different ratios between the Gaussian noise and the Poisson noise. The problems so obtained have a relative noise level $\|\boldsymbol{\eta}\|/\|A\boldsymbol{x}^*\|$ ranging from 0.9% to 7% for the galaxy, from 1.2% to 9.7% for the satellite, from 2.8% to 12% for the Shepp-Logan phantom and from 0.7% to 5.8% for the Hoffman phantom. The ratio between the two types of noises (Gaussian and Poisson)varies from 0 to 1.5.

Each problem is solved using the three algorithms and for each algorithm the error history $\epsilon^{(k)}$ is recorded. The optimal index $K$, corresponding to the minimum of the error history, is computed, together with the optimal error $\epsilon^{(K)}$. The trace of $A_k$ is also computed, by using only procedure $\mathbf{P}_1$ for EM, and both procedures $\mathbf{P}_1$ and $\mathbf{P}_2$ for WMRNSD and SGP. The ten stopping rules $\mathbf{S}_j$, $j = 1, \ldots, 10$, are applied and the stopping indices $K_j$ are detected. The indicators

$$e_j = \frac{\epsilon^{(K_j)}}{\epsilon^{(K)}} - 1 \geq 0, \quad d_j = \frac{K_j}{K} - 1, \quad f_j = |d_j|$$

measure the effectiveness of the $j$th rule. The lower $e_j$ and $f_j$, the more effective the $j$th rule. The sign of $d_j$ allows discriminating between an early and a late stop. The quantities $e_j^{av}$ and $f_j^{av}$, obtained by averaging $e_j$ and $f_j$ on all the problems, are shown in the tables which summarize the results of the experiments.

A first set of experiments compares the effects of the two procedures $\mathbf{P}_1$ and $\mathbf{P}_2$ for what concerns the rules which make use of the trace. For both WMRNSD and SGP the results are comparable for all the levels of the noise, showing that the derivatives with respect to $\boldsymbol{b}$ of the step sizes are in fact negligible. In the following we show the results obtained with procedure $\mathbf{P}_1$.

A second set of experiments compares the performance of the functionals $GCV$ and $U$ given in (18) and (20) with the performance of the weighted functionals $GCV_W$ and $U_W$ given in (19) and (21). There is a large majority of negative signs of $d_j$, corresponding to early stops. Late stops arise only in some cases where $K_j$ is small. Table 1 lists in percentage the averages $e_j^{av}$ and $f_j^{av}$ for $j = 1, \ldots, 4$.

We note that the average errors on the stopping index are two digits figures, but the corresponding indicators $e_j$ are reasonably small. This is a consequence of the flat shape of the error history $\epsilon^{(k)}$, which characterizes methods with a low convergence rate. In fact, the indicator $f_j$ of SGP, noticeably smaller than those of EM and WMNRSD, corresponds to a higher

| Method | $e_1^{av}$ | $e_2^{av}$ | $e_3^{av}$ | $e_4^{av}$ | $f_1^{av}$ | $f_2^{av}$ | $f_3^{av}$ | $f_4^{av}$ |
|---|---|---|---|---|---|---|---|---|
| EM | 0.45 | 1.21 | 0.43 | 1.22 | 26.9 | 40.1 | 26.9 | 40.3 |
| WMNRSD | 0.58 | 1.29 | 0.58 | 1.32 | 28.8 | 39.1 | 28.7 | 39.3 |
| SGP | 0.49 | 1.21 | 0.48 | 1.24 | 16.4 | 25.6 | 16.2 | 26.6 |

Table 1: Average measures in percentage of the effectiveness of the stopping rules based on estimates of the predictive error.

convergence rate, hence to a steeper shape of $\epsilon^{(k)}$. In the following tables the indicators $f_j$ are shown for the sake of completeness, even if their role is marginal.

In any case $e_1^{av} < e_2^{av}$ and $e_3^{av} < e_4^{av}$. Hence the nonweighted functionals outperform the weighted functionals, suggesting that the use of the latter ones should be restrict to the cases where the oscillations of the former ones prevent a correct detection of the minimum point. Table 1 shows also that $\mathbf{S}_3$ slightly outperforms $\mathbf{S}_1$. As a matter of fact, the mean of the differences $|e_1 - e_3|$ on all the problems results approximately 0.05, confirming what is generally stated in the literature, i. e. that the behaviors of CGV and UPRE are closely related when a good estimate of $\sigma$ is availale. In our context UPRE appears to be the most suitable rule for methods which already exploit the knowledge of $\sigma$ like WMNRSD. Otherwise GCV, which does not require the knowledge of $\sigma$, should be used.

A third set of experiments examines the performance of the stopping rules based on the discrepancy principle, comparing the rules $\mathbf{S}_5$, $\mathbf{S}_6$ and $\mathbf{S}_7$ which do not use the trace of $A_k$ with the corresponding rules $\mathbf{S}_8$, $\mathbf{S}_9$ and $\mathbf{S}_{10}$ which use the trace. The signs of $d_j$ are all negative for $\mathbf{S}_5$, $\mathbf{S}_6$ and $\mathbf{S}_7$, and are negative in a large majority for $\mathbf{S}_8$, $\mathbf{S}_9$ and $\mathbf{S}_{10}$. This indicates that the stopping rules based on the discrepancy principle lead often to early stops. Table 2 lists in percentage the averages $e_j^{av}$ and $f_j^{av}$ for $j = 5, \ldots, 10$. The rules which do not use the trace appear to perform poorly with respect to the corresponding trace based rules. This result confirms that the introduction of a more realistic estimate of the degrees of freedom improves the statistical inferences and that the use of trace based rules is suggested, despite the doubling of the cost.

A fourth set of experiments aims at comparing the performance of rule $\mathbf{S}_{10}$ with respect to $\mathbf{S}_8$ and $\mathbf{S}_9$. We expect that $\mathbf{S}_{10}$ takes advantage from a prevailing Poisson component of the noise distribution. For this reason problems without Gaussian noise have been generated (see the results in Table 3). It appears that when the noise is of Poisson type, rule $\mathbf{S}_{10}$ is outperformed by $\mathbf{S}_8$ and outperforms $\mathbf{S}_9$ only when coupled with WMNRSD.

| Method | $e_5^{av}$ | $e_6^{av}$ | $e_7^{av}$ | $e_8^{av}$ | $e_9^{av}$ | $e_{10}^{av}$ |
|---|---|---|---|---|---|---|
| EM | 8.01 | 9.82 | 10.1 | 2.22 | 3.39 | 4.08 |
| WMNRSD | 8.56 | 10.6 | 10.6 | 2.27 | 4.04 | 3.90 |
| SGP | 9.01 | 11.1 | 11.5 | 2.92 | 4.05 | 4.64 |

| Method | $f_5^{av}$ | $f_6^{av}$ | $f_7^{av}$ | $f_8^{av}$ | $f_9^{av}$ | $f_{10}^{av}$ |
|---|---|---|---|---|---|---|
| EM | 82.4 | 84.9 | 85.4 | 52.6 | 60.8 | 64.7 |
| WMNRSD | 80.9 | 83.5 | 83.5 | 51.4 | 62.5 | 61.3 |
| SGP | 63.8 | 67.1 | 67.6 | 38.5 | 44.3 | 47.6 |

Table 2: Average measures in percentage of the effectiveness of the stopping rules based on the discrepancy principle.

| Method | $e_8^{av}$ | $e_9^{av}$ | $e_{10}^{av}$ | $f_8^{av}$ | $f_9^{av}$ | $f_{10}^{av}$ |
|---|---|---|---|---|---|---|
| EM | 1.87 | 3.26 | 4.28 | 52.1 | 60.2 | 65.5 |
| WMNRSD | 1.54 | 3.93 | 3.75 | 45.5 | 61.5 | 59.8 |
| SGP | 3.75 | 4.04 | 4.88 | 42.6 | 44.5 | 48.6 |

Table 3: Average measures in percentage of the effectiveness of the stopping rules based on the discrepancy principle for problems without Gaussian noise.

The comparison of the values of Table 2 shows that on average $\mathbf{S}_8$ outperforms both $\mathbf{S}_9$ and $\mathbf{S}_{10}$. For a more detailed comparison between $\mathbf{S}_8$ and $\mathbf{S}_9$, the following functions of the iteration index are examined

$$\tau(k) = N - \text{tr } A_k, \quad \rho_8(k) = \frac{N\|\boldsymbol{r}^{(k)}\|^2}{\sum_i (b_i + \sigma^2)}, \quad \rho_9(k) = \|W^{1/2}\boldsymbol{r}^{(k)}\|^2.$$

Figure 1 shows a typical situation: the plots versus $k$ of $\rho_8(k)$ and $\rho_9(k)$ cross the plot of $\tau(k)$ at indices $k_8$ and $k_9$ respectively (in the figure $k_9 < k_8$, but the opposite situation may occur). The position of the optimal index $K$ establishes which rule is the best one.

In most our experiments $k_9 < k_8 < K$, thus rule $\mathbf{S}_8$ outperforms $\mathbf{S}_9$, but in some cases $k_8 < k_9 < K$, thus rule $\mathbf{S}_9$ outperforms $\mathbf{S}_8$. For the Shepp-Logan image this occurs in one-fourth of the problems solved with EM and SGP (but never with WMNRSD), mainly when the Poisson noise is large and prevailing on the Gaussian noise.

Finally, we compare the performances of the rules $\mathbf{S}_1$ and $\mathbf{S}_3$ (based on the predictive error) and $\mathbf{S}_8$, $\mathbf{S}_9$ and $\mathbf{S}_{10}$ (based on the discrepancy principle). Figure 2 shows $e_j$ versus $\epsilon^{(K)}$ for all the problems solved by the three methods EM, WMNRSD and SGP. The black points refer to $\mathbf{S}_1$ and $\mathbf{S}_3$, the

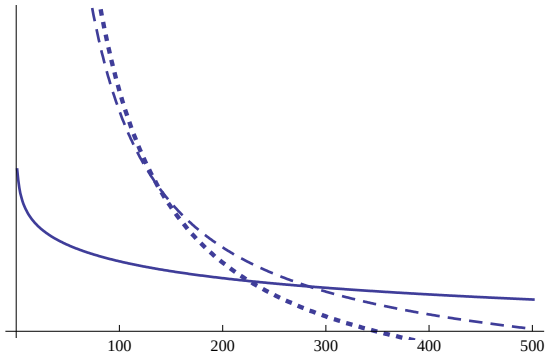


Figure 1: Plots of $\tau(k)$ (solid line), $\rho_8(k)$ (dashed line) $\rho_9(k)$ (dotted line)

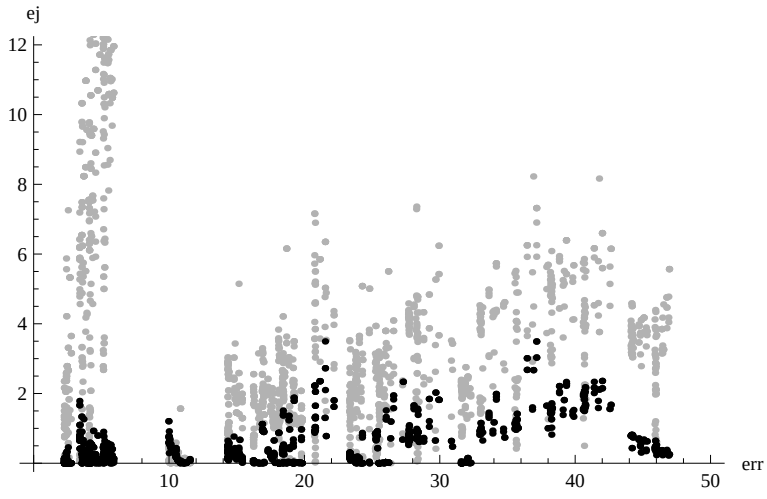


Figure 2: Error indicators $e_j$ for $\mathbf{S}_1$, $\mathbf{S}_3$ (black points) and for $\mathbf{S}_8$, $\mathbf{S}_9$, $\mathbf{S}_{10}$ (gray points) versus optimal errors $\epsilon^{(K)}$

gray points refer to $\mathbf{S}_8$, $\mathbf{S}_9$ and $\mathbf{S}_{10}$. Rules $\mathbf{S}_1$ and $\mathbf{S}_3$ appear to have a better performance, independently from the optimal errors. In particular, the difference between the gray points and the black points result to be very large for small values of $\epsilon^{(K)}$, which correspond to the galaxy problem. In general the rules based on the discrepancy principle tend to stop too early. But an early stop can be advantageous, since it leads to a reduction of the global computational cost, provided that the error history varies slowly enough to allow acceptable errors. Moreover we must take into consideration that detecting the crossing point of two curves is in general an easier task than evaluating a minimum, especially when there are oscillations.

# 8 Conclusions

Ten stopping rules $\mathbf{S}_j$, $j = 1, \ldots, 10$ have been considered for iterative methods in the nonnegatively constrained deconvolution of images. Two averaged indicators $e_j^{av}$ and $f_j^{av}$ have been introduced to measure the effectiveness of the $j$th rule. Because of the experimental nature of the analysis we have performed, it is obviously impossible to rate these rules, but some considerations can be drawn.

1. The computation of the trace of the influence matrix for a reliable determination of the degree of freedom can be well performed both analytically (using formal derivatives) and approximately (exploiting the different quotient). The rules which use the trace are more effective than those which do not use it, despite the doubling of the cost.

2. The rules which require the knowledge of $\sigma$, like UPRE and those based on the discrepancy principle, are more suitable in connection with methods which already make use of $\sigma$, like WMNRSD. Otherwise GCV, which does not use $\sigma$, offers a reliable alternative.

3. The rules based on the predictive error averagely outperform those based on the discrepancy principle.

# References


[1] J.M. Bardsley, *Stopping Rules for a Nonnegatively Constrained Iterative Method for Ill-Posed Poisson Imaging Problems*, BIT Numerical Mathematics, **46**, 2008, pp. 651-664.

[2] J.M. Bardsley and J. Goldes, *Regularization parameter selection methods for ill-posed Poisson maximum likelihood esitimation*, Inverse Problems, **25**, 2009, 095005.

[3] J.M. Bardsley and J.G. Nagy, *Covariance-preconditioned iterative methods for nonnegatively constrained astronomical imaging*, Siam J. Matrix Anal. Appl., **27**, 2006, pp. 1184-1197.

[4] F. Bauer and M.A. Lukas, *Comparing parameter choice methods for regularization of ill-posed problems*, Mathematics and Computers in Simulation, **81**, 2011, pp. 1795-1841.

[5] M. Bertero and P. Boccacci, *Introduction to Inverse Problems in Imaging*, Institute of Physics Publishing, Bristol, 1988.

[6] *Image restoraton methods for the Large Binocular Telescope (LBT)*, Astron. Astrophys. Suppl. Ser. **147**, 2000, pp. 323-333.

[7] S. Bonettini, R. Zanella and L. Zanni, *A Scaled Gradient Projection Method for Constrained Image Deblurring*, Inverse Problem, **25**, 2009, 015002.

[8] P. Favati, G. Lotti, O. Menchi and F. Romani, *Performance analysis of maximum likelihood methods for regularization problems with nonnegativity constraints*, Inverse Problems, **26**, 2010, 085013.

[9] P.C. Hansen, *Rank-Deficient and Discrete Ill-Posed Problems* SIAM Monographs on Mathematical Modeling and Computation, Philadelphia, 1998.

[10] E.J. Hoffman, P.D. Cutler, W.M. Digby and J.C. Mazziotta, *3-D phantom to simulate cerebral blood flow and metabolic images for PET*, IEEE Trans. Nucl. Sci., **37**, 1990 , pp. 616-620.

[11] K.P. Lee, J.G. Nagy and L. Perrone *Iterative methods or image restoration: a Matlab object oriented approach*, 2002 http://www.mathcs.emory.edu/∼nagy/RestoreTools

[12] K.M. Perry and S.J. Reeves, *Generalized Cross-Validation as a Stopping Rule for the Richardson-Lucy Algorithm*, in The Restoration of HST Images and Spectra II. R.J. Hanisch and R.L. White, Eds., Space Telescope Science Institute, 1994, pp. 97-103.

[13] K.M. Perry and S.J. Reeves, *A Practical Stopping Rule for Iterative Signal Restoration*, IEEE Transaction on Signal Processing, **42**, 1994, pp. 1829-1933.

[14] A.M. Thomson, J.C. Brown, J.W. Kay and D.M. Titterington, *A study of Methods of Choosing the Smoothing Parameter in Image Restoration by Regularization*, IEEE Trans. on Pattern Analysis and Machine Intelligence, **13**, 1991, pp. 326-339.

[15] C.R. Vogel, *Computational Methods for Inverse Problems*, SIAM Frontier in Applied Mathematics, Philadelphia, 2002.

[16] R. Zanella, P. Boccacci, L. Zanni and M. Bertero, *Efficient gradient projection methods for edge-preserving removal of Poisson noise*, Inverse Problems, **25**, 2009, 045010.

[17] http://www.oersted.dtu.dk/ftp/jaj/31655/ct_programs/